



# Mapping the differential reddening in globular clusters

C. Bonatto, F. Campos, and S. O. Kepler

Departamento de Astronomia – Universidade Federal do Rio Grande do Sul, Av. Bento Gonçalves 9500, Porto Alegre 91501-970, RS, Brazil  
e-mail: charles.bonatto@ufrgs.br

**Abstract.** Differential-reddening maps for 66 Galactic globular clusters (GCs) are built with archival HST WFC/ACS F606W and F814W photometry. We divide the WFC/ACS field of view across each cluster in a regular cell grid and extract the stellar-density Hess diagram from each cell. Shifts in colour and magnitude along the reddening vector are applied until a match with the mean diagram is obtained. The maps correspond to the internal dispersion of the reddening around the mean. We detect spatially-variable extinction in the 66 globular clusters studied, with mean values ranging from  $\langle \delta E(B - V) \rangle \approx 0.018$  (NGC 6981) up to  $\langle \delta E(B - V) \rangle \approx 0.16$  (Palomar 2). Differential-reddening correction decreases the observed foreground reddening and the apparent distance modulus but, since they are related to the same value of  $E(B - V)$ , the distance to the Sun is conserved. While the foreground  $E(B - V)$  increases rather steeply towards the Galactic plane,  $\langle \delta E(B - V) \rangle$  does the same with a much flatter slope, thus suggesting that part of the measured DR originates inside the clusters. However, the lack of systematic variations of  $\langle \delta E(B - V) \rangle$  with the sampled cluster area indicates that most of the differential reddening is interstellar.

**Key words.** (*Galaxy:*) globular clusters: general

## 1. Introduction

Spatially-variable extinction, or differential reddening (DR), occurs in all directions throughout the Galaxy and is also present across the field of view of most globular clusters (GCs). By introducing non-systematic confusion in the actual colour and magnitude of member stars located in different parts of a GC, it leads to a broadening of evolutionary sequences in the colour-magnitude diagram (CMD). Thus, together with significant photometric scatter, unaccounted-for DR hampers the detection of multiple-population se-

quences and may difficult the precise determination of fundamental parameters of GCs.

We assume that, if DR is non negligible, CMDs extracted in different parts of a GC would be similar to each other but shifted along the reddening vector by an amount proportional to the relative extinction between the regions. Thus, residual minimization by matching CMDs can be used to search for the extinction values affecting different places of a GC. The 66 GCs focused here are part of the HST Treasury project in which a large sample of GCs was observed through the F606W and F814W filters (Milone et al. 2012; Dotter, Sarajedini & Anderson 2011).

---

Send offprint requests to: C. Bonatto

## 2. The approach and results

The projected stellar distribution of member stars is divided in a grid of cells, and the CMD of each cell is extracted and converted into a Hess diagram (Hess 1924). As constraint, we only consider cells having a number of stars higher than a minimum value  $N_{min}$  according to:  $50 \leq N_{min} \leq 150$ , higher for the GCs with more detected stars. The spatial grids range from  $10 \times 10$  to  $30 \times 30$ , with the resolution increasing with the number of stars. Thus, the angular resolution of the DR maps range from  $\approx 7'' \times 7''$  to  $\approx 20'' \times 20''$ . Then, we search for the optimum value of  $\delta E(B - V)$  that leads to the best match between the Hess diagram of a cell and that of the whole distribution, which is equivalent to computing the reddening dispersion around the mean, since a differentially-reddened GC should contain cells bluer and redder than the mean. Axes of the reddening vector have amplitudes corresponding to the absorption relations  $A_{F606W} = 2.86\delta E(B - V)$  and  $A_{F814W} = 1.88\delta E(B - V)$ . Finally, we compute the difference in reddening between each cell and the bluest one, which also leads to the DR maps and the DR-corrected CMDs.

Because it is relatively time efficient, robust and capable of finding the optimum minimum, residuals are minimised with Adaptive Simulated Annealing (e.g. Goffe, Ferrier & Rogers 1994; Bonatto, Lima & Bica 2012; Bonatto & Bica 2012). This process is partially illustrated in Fig. 1, in which the Hess diagrams of the bluest and reddest cells of NGC 6388 are compared to the overall/mean one. Except for the evolved sequences (and the relative stellar density), the bluest and reddest cell diagrams have similar morphologies, differing somewhat in magnitude and colour.

The DR maps shown in Fig. 2 are typical among our GC sample. They show that extinction may be patchy (as in the centre of NGC 6715) and scattered (as across Terzan 8), rather uniform (as in Palomar 2, where it is apparently distributed as a thin dust cloud lying along the north-south direction), or somewhat defining a gradient (like in NGC 104).

Our approach detects some measurable amount of DR in the 66 GCs dealt with in

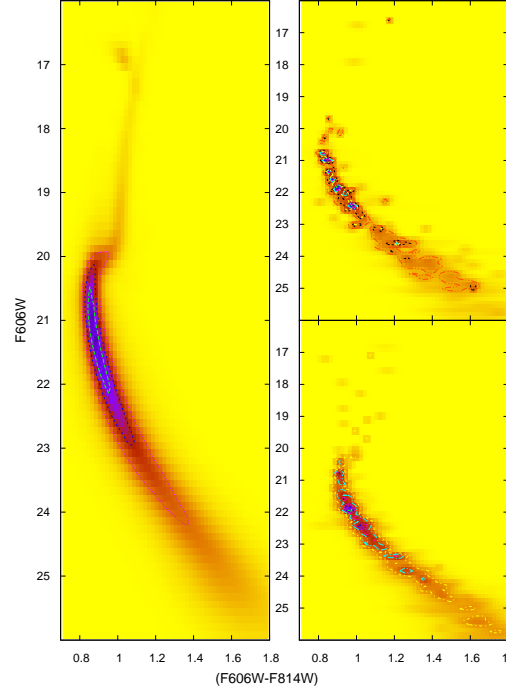


**Fig. 1.** The bluest (top-right panel) and reddest (bottom-right) Hess diagrams of NGC 6388 are compared to the mean (observed) one (left). The difference in reddening between both amounts to  $\delta E(B - V) = 0.133$ .

this paper. To summarize this point, we show in Fig. 3 the distribution function (DF) of the  $\delta E(B - V)$  measured over all cells of selected GCs, from which the mean and maximum DR values,  $\langle \delta E(B - V) \rangle$  and  $\delta E(B - V)_{max}$ , can be measured. Some GCs, like NGC 104, NGC 2808, NGC 5286, and NGC 6715, have roughly log-normal DFs, while in others like Palomar 2, the DFs are flat and broad. The majority (67%) of the GCs have the mean DR characterized by  $\langle \delta E(B - V) \rangle \lesssim 0.04$ , with the highest value  $\langle \delta E(B - V) \rangle = 0.161$  occurring in Palomar 2. Regarding the maximum DR value, 67% of the GCs have  $\delta E(B - V)_{max} \lesssim 0.09$ , with the highest  $\delta E(B - V)_{max} = 0.375$  again in Palomar 2.

Finally, in Fig. 4 we study dependences and correlations among the derived parameters. The three reddening parameters appear to anti-

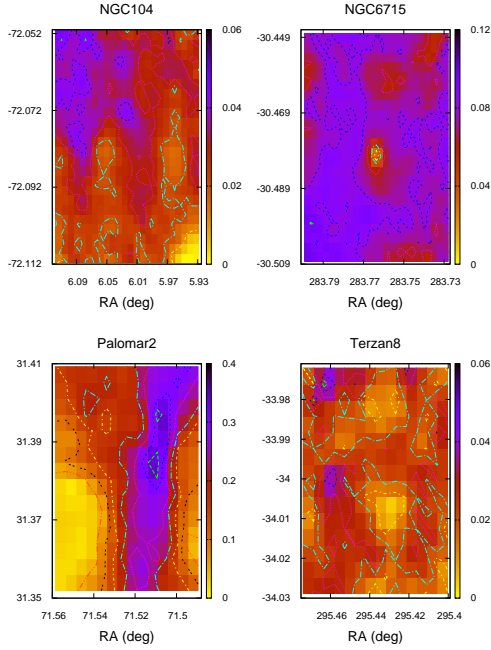


**Fig. 2.** Differential-reddening maps of NGC 104, NGC 6715, Palomar 2 and Terzan 8. The range of values of  $\delta E(B - V)$  is shown by the colour bars.

correlate with the distance to the Galactic plane (top-left panel) at very different degrees. As expected, the foreground absorption  $E(B - V)$  clearly increases towards the Galactic plane ( $|b|$ ) according to  $E(B - V) = (1.59 \pm 0.44) \times |b|^{-(0.78 \pm 0.13)}$ , with the mild correlation coefficient  $CC = 0.63$ . A similar, but shallower dependence occurs for the maximum DR,  $\delta E(B - V)_{max} = (0.24 \pm 0.05) \times |b|^{-(0.40 \pm 0.08)}$ , with  $CC = 0.48$ . However, the mean DR values present a weaker dependence on  $|b|$ ,  $\langle \delta E(B - V) \rangle = (0.05 \pm 0.01) \times |b|^{-(0.14 \pm 0.06)}$ , with  $CC = 0.28$ . The weak and flat dependence of  $\langle \delta E(B - V) \rangle$  with  $|b|$ , in particular, suggests that part of the measured DR originates inside the clusters, otherwise, the mean DR should increase towards the plane with a similar slope as the foreground  $E(B - V)$ .

Both  $\delta E(B - V)_{max}$  and  $\langle \delta E(B - V) \rangle$  are similarly uncorrelated with the angular distance to the Galactic centre ( $|\Delta\ell|$ ); the same

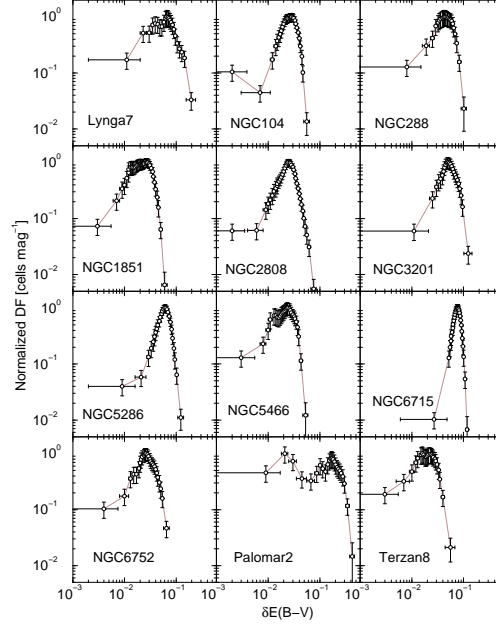


**Fig. 3.** Distribution function of  $\delta E(B - V)$  for a representative GC sub-sample. For comparison purposes, the DFs are normalized by the peak.

occurs with the foreground  $E(B - V)$ , but with the scatter having larger amplitude (top-right panel). Regarding the dependence on the foreground  $E(B - V)$ , both the mean and maximum DR values appear to correlate only for  $E(B - V) \gtrsim 0.2$  (bottom-left panel). Indeed, the best representation for both is a straight line, with a strong correlation for the maximum DR  $\delta E(B - V)_{max} = (0.043 \pm 0.004) + (0.20 \pm 0.01) \times E(B - V)$ , with  $CC = 0.85$ , while the mean DR is only mildly correlated,  $\langle \delta E(B - V) \rangle = (0.026 \pm 0.002) + (0.04 \pm 0.01) \times E(B - V)$ , with  $CC = 0.45$ . This probably implies that reddening internal to the clusters is the main source of DR when the foreground extinction is  $E(B - V) \lesssim 0.2$ . Consequently, interstellar (external) reddening dominates the DR for higher values of  $E(B - V)$ .

The issue concerning the internal/external to the clusters nature of the differential-reddening source can be investigated from another perspective. Although the fraction of the cluster area covered by WFC/ACS  $S \equiv R_{obs}/R_h$  varies significantly among our sam-

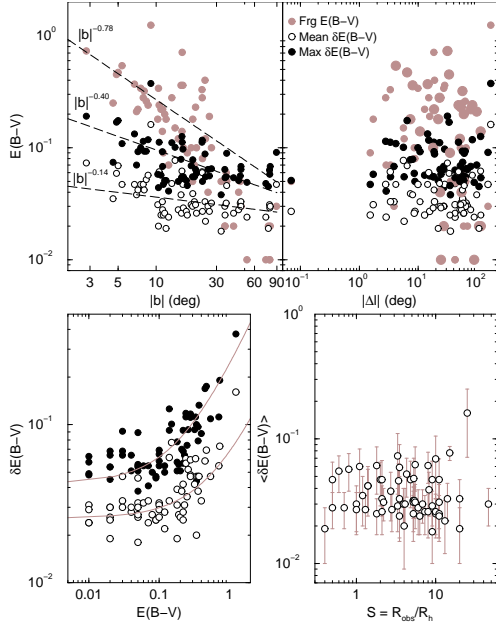


**Fig. 4.** Reddening parameters as a function of the angular distance to the Galactic plane (top-left), and to the centre (top-right). The dependence on  $|b|$  is characterized by power-laws (dashed lines).  $\delta E(B-V)_{max}$  and  $\langle \delta E(B-V) \rangle$  are mildly correlated with  $E(B-V)$  (bottom-left). There is no correlation between  $\langle \delta E(B-V) \rangle$  and the GC area covered by WFC/ACS (bottom-right).

ple, its effect on the mean DR values is essentially negligible (Fig. 4, bottom-right). A reasonable assumption is that, if the source of DR is essentially internal to the clusters, with the dust distribution following the cluster stellar structure, differences in  $\delta E(B-V)$  - and thus the mean DR - should increase with  $S$ . In this context, while the different dependence of  $E(B-V)$  and  $\langle \delta E(B-V) \rangle$  with distance to the Galactic plane and the straight-line relation between both point to a shared origin for the DR, the lack of a systematic variation of  $\langle \delta E(B-V) \rangle$  with  $S$  indicates that most of the DR source is external to the clusters.

### 3. Conclusions

We derive the DR maps of 66 Galactic globular clusters from archival HST WFC/ACS

data uniformly observed with the F606W and F814W filters. The maps have angular resolutions in the range  $\approx 7'' \times 7''$  to  $\approx 20'' \times 20''$ . According to current census (e.g. Ortolani et al. 2012), our sample contains  $\sim 40\%$  of the Milky Way's GC population, which implies that the results can be taken as statistically significant.

We find spatially-variable extinction in the 66 GCs, with mean values (with respect to the cell to cell distribution) ranging from  $\langle \delta E(B-V) \rangle \approx 0.018$  (NGC 6981) up to  $\langle \delta E(B-V) \rangle \approx 0.16$  (Palomar 2). By comparing dependences of the foreground and DR-related parameters with the distance to the Galactic plane, we suggest that part of the  $\delta E(B-V)$  extinction is internal to the GCs. However, the lack of systematic variations of the mean-DR values with the cluster area sampled by WFC/ACS indicates that most of the differential reddening is interstellar, especially when the foreground extinction is relatively high,  $E(B-V) \gtrsim 0.2$ .

*Acknowledgements.* Partial financial support for this research comes from CNPq, PRONEX-FAPERGS/CNPq and PROPESQ/UFRGS (Brazil). Data used in this paper are from *The ACS Globular Cluster Survey*: [http://www.astro.ufl.edu/~ata/public\\_hstgc/](http://www.astro.ufl.edu/~ata/public_hstgc/).

### References

- Bonatto C. & Bica E. 2012, MNRAS, 423, 1390
- Bonatto C., Lima E.F. & Bica E. 2012, A&A, 540A, 137
- Dotter A., Sarajedini A. & Anderson J. 2011, ApJ, 738, 74
- Goffe W.L., Ferrier G.D. & Rogers J. 1994, Journal of Econometrics, 60, 65
- Hess R. 1924, in *Die Verteilungsfunktion der absol. Helligkeiten etc.* Probleme der Astronomie. Festschrift für Hugo v. Seeliger. (Berlin:Springer), 265
- Milone A.P., et al. 2012, A&A, 540A, 16
- Ortolani S., Bonatto C., Bica E., Barbuy B. & Saito R.K. 2012, AJ, 144, 147